



NAVAL POSTGRADUATE SCHOOL

MONTEREY, CALIFORNIA

THESIS

**CHARACTERIZATION OF THE VERTICAL
STRUCTURE OF TIDAL CURRENTS IN THE GOLDEN
GATE (SAN FRANCISCO) INLET**

by

Muhammad Khalid

December 2012

Thesis Advisor:
Second Reader:

Thomas Herbers
James MacMahan

Approved for public release; distribution is unlimited

THIS PAGE INTENTIONALLY LEFT BLANK

REPORT DOCUMENTATION PAGE			<i>Form Approved OMB No. 0704-0188</i>	
Public reporting burden for this collection of information is estimated to average 1 hour per response, including the time for reviewing instruction, searching existing data sources, gathering and maintaining the data needed, and completing and reviewing the collection of information. Send comments regarding this burden estimate or any other aspect of this collection of information, including suggestions for reducing this burden, to Washington headquarters Services, Directorate for Information Operations and Reports, 1215 Jefferson Davis Highway, Suite 1204, Arlington, VA 22202-4302, and to the Office of Management and Budget, Paperwork Reduction Project (0704-0188) Washington, DC 20503.				
1. AGENCY USE ONLY (Leave blank)		2. REPORT DATE December 2012	3. REPORT TYPE AND DATES COVERED Master's Thesis	
4. TITLE AND SUBTITLE CHARACTERIZATION OF THE VERTICAL STRUCTURE OF TIDAL CURRENTS IN THE GOLDEN GATE (SAN FRANCISCO) INLET			5. FUNDING NUMBERS	
6. AUTHOR(S) Muhammad Khalid				
7. PERFORMING ORGANIZATION NAME(S) AND ADDRESS(ES) Naval Postgraduate School Monterey, CA 93943-5000			8. PERFORMING ORGANIZATION REPORT NUMBER	
9. SPONSORING /MONITORING AGENCY NAME(S) AND ADDRESS(ES) N/A			10. SPONSORING/MONITORING AGENCY REPORT NUMBER	
11. SUPPLEMENTARY NOTES The views expressed in this thesis are those of the author and do not reflect the official policy or position of the Department of Defense or the U.S. Government. IRB Protocol number ____ N/A ____.				
12a. DISTRIBUTION / AVAILABILITY STATEMENT Approved for public release; distribution is unlimited			12b. DISTRIBUTION CODE A	
13. ABSTRACT (maximum 200 words) <p>In the Golden Gate (San Francisco) inlet, tidal currents are dominant and have complex spatial and temporal variations owing to the large size of estuary connected through a narrow channel and the shallow ebb shoal (bar) at the mouth. To capture such variations, shipboard ADCP profiling is a technically viable approach that can yield unique insight into the vertical structure of currents. Shipboard ADCP data from four cruises conducted by the R/V Point Sur in the San Francisco Bight are used in the study. Transects along the channel axis were automatically extracted from the irregularly sampled underway data using changes in speed and heading in combination with geographic criteria.</p> <p>Processed data contains transects traversed in various tidal conditions. Flood currents are bottom intensified with more strength in the relatively deeper area of the channel. In low tidal range conditions, the directions and speed of surface currents are nearly uniform along the entire channel. Ebb currents are surface intensified, decreasing from the Golden Gate to the bar. In low tidal range, near-surface and bottom currents flow in opposite directions. The tidal currents exhibit cross channel variations in strength. Ebb results in surface outflow mainly along the northern part of entrance, whereas the flood flow is strongest along the southern part.</p>				
14. SUBJECT TERMS ADCP, Golden Gate, San Francisco Bay, Tidal currents			15. NUMBER OF PAGES 65	
			16. PRICE CODE	
17. SECURITY CLASSIFICATION OF REPORT Unclassified	18. SECURITY CLASSIFICATION OF THIS PAGE Unclassified	19. SECURITY CLASSIFICATION OF ABSTRACT Unclassified	20. LIMITATION OF ABSTRACT UU	

THIS PAGE INTENTIONALLY LEFT BLANK

Approved for public release; distribution is unlimited

**CHARACTERIZATION OF THE VERTICAL STRUCTURE OF TIDAL
CURRENTS IN THE GOLDEN GATE (SAN FRANCISCO) INLET**

Muhammad Khalid
Commander, Pakistan Navy
B.Sc (Hons.) (Naval Sciences), University of Karachi, 1996
Postgraduate Diploma in Hydrography, University of Plymouth, 2003

Submitted in partial fulfillment of the
requirements for the degree of

MASTER OF SCIENCE IN PHYSICAL OCEANOGRAPHY

from the

**NAVAL POSTGRADUATE SCHOOL
December 2012**

Author: Muhammad Khalid

Approved by: Thomas Herbers
Thesis Advisor

James MacMahan
Second Reader

Peter Chu
Chair, Department of Oceanography

THIS PAGE INTENTIONALLY LEFT BLANK

ABSTRACT

In the Golden Gate (San Francisco) inlet, tidal currents are dominant and have complex spatial and temporal variations owing to the large size of estuary connected through a narrow channel and the shallow ebb shoal (bar) at the mouth. To capture such variations, shipboard ADCP profiling is a technically viable approach that can yield unique insight into the vertical structure of currents. Shipboard ADCP data from four cruises conducted by the R/V Point Sur in the San Francisco Bight are used in the study. Transects along the channel axis were automatically extracted from the irregularly sampled underway data using changes in speed and heading in combination with geographic criteria.

Processed data contains transects traversed in various tidal conditions. Flood currents are bottom intensified with more strength in the relatively deeper area of the channel. In low tidal range conditions, the directions and speed of surface currents are nearly uniform along the entire channel. Ebb currents are surface intensified, decreasing from the Golden Gate to the bar. In low tidal range, near-surface and bottom currents flow in opposite directions. The tidal currents exhibit cross channel variations in strength. Ebb results in surface outflow mainly along the northern part of entrance, whereas the flood flow is strongest along the southern part.

THIS PAGE INTENTIONALLY LEFT BLANK

TABLE OF CONTENTS

I.	INTRODUCTION.....	1
A.	MOTIVATION AND BACKGROUND	1
B.	RESEARCH QUESTIONS.....	3
1.	Primary Research Question	3
2.	Subsidiary Research Questions	3
C.	CONTRIBUTIONS.....	3
D.	THESIS ORGANIZATION.....	3
II.	BACKGROUND	5
A.	SHALLOW WATER CURRENTS.....	5
1.	Tides and Tide-Driven Currents	5
2.	Non-Tidal Currents	6
3.	Time Scales of Tide, Wind and Density Driven Currents	6
B.	SAN FRANCISCO BAY AND GOLDEN GATE AREA.....	7
1.	San Francisco Bay	7
2.	Bathymetric Features of Golden Gate and Offshore Area	8
3.	Tides and Tidal Currents	10
a.	<i>Character of Tide and Tidal Currents.....</i>	<i>11</i>
b.	<i>Spatial Variability of Tidal Currents.....</i>	<i>13</i>
4.	Modeling of tidal currents of San Francisco Bay	14
C.	MEASUREMENT OF CURRENTS	15
1.	ADCP Basic Principle.....	16
2.	Accuracy and Limitations of ADCP Measurements.....	19
3.	Applications of Shipboard ADCP Data Collection	20
III.	DATA AND METHODOLOGY	21
A.	DATA COLLECTION AND PROCESSING ONBOARD SHIP.....	21
1.	ADCP Arrangement on Ship	21
2.	Overview of Data Collection and Onboard Processing	21
3.	Detail of Collected Data.....	22
B.	DATA PROCESSING METHODOLOGY	23
1.	Extraction of Transects	23
a.	<i>Overview of the Transect Extraction Methodology</i>	<i>24</i>
b.	<i>Overview of the Matlab Processing.....</i>	<i>25</i>
2.	Post Processing/Editing of Data.....	27
IV.	RESULTS	29
A.	FLOOD CURRENT CASE.....	30
1.	LOW RANGE FLOOD	30
2.	HIGH RANGE FLOOD	32
B.	EBB CURRENT CASE	34
1.	LOW RANGE EBB	34
2.	HIGH RANGE EBB	36
C.	CROSS-CHANNEL VARIATION IN CURRENT STRENGTH.....	38

V.	CONCLUSION	41
A.	SUMMARY	41
B.	FUTURE RESEARCH.....	42
	LIST OF REFERENCES	43
	INITIAL DISTRIBUTION LIST	47

LIST OF FIGURES

Figure 1.	San Francisco Bay and region of interest in Red rectangle (From Trump, 2008)	2
Figure 2.	Time scales of different current driving mechanisms (From MetEd COMET Program)	7
Figure 3.	Geography of San Francisco Bay (From Grove, 2001)	8
Figure 4.	Bathymetry of Golden Gate and adjacent offshore area (From Barnard, 2005)	9
Figure 5.	Oblique view of the giant sand waves and other bed forms at the mouth of San Francisco Bay (From Barnard, Hanes, Rubin, & Kvitek, 2006).....	10
Figure 6.	Tidal Data of San Francisco Bay (From Cheng & Gartner, 1984)	12
Figure 7.	Comparison of sea level and current (7–10 January 2010) at Golden Gate (After NOAA Tides and Currents, 2012)	13
Figure 8.	PORTS sensor locations map (left) and current product (right) (From Cheng & Smith, 1998)	14
Figure 9.	The relationship of beam and earth velocity components (From Teledyne RD Instruments, 1996).....	17
Figure 10.	Ship tracks during ADCP data collection	22
Figure 11.	Example histograms of Speed and Headings.....	25
Figure 12.	Geographical location of final extracted transects.....	27
Figure 13.	Current strength data before and after applying ‘last good bin (lgb)’ filter.....	28
Figure 14.	Low Range Flood Cycle (27 April 2012)	31
Figure 15.	High Range Flood Cycle (17 October 2012)	33
Figure 16.	Low Range Ebb Cycle (27 April 2012)	35
Figure 17.	High Range Ebb Cycle (15 February 2012)	37
Figure 18.	Cross Channel Variation of Currents (18 October 2012)	39

THIS PAGE INTENTIONALLY LEFT BLANK

LIST OF TABLES

Table 1.	Important Tidal Datums-San Francisco (NOAA Datums-San Francisco)12
----------	--

THIS PAGE INTENTIONALLY LEFT BLANK

LIST OF ACRONYMS AND ABBREVIATIONS

CTD	Conductivity Temperature Depth
DGPS	Differential Global Positioning System
HW	High Water
LW	Low Water
MHW	Mean High Water
MHHW	Mean Higher High Water
MLLW	Mean Lower Low Water
MTL	Mean Tide Level
MLW	Mean Low Water
NEFSC	Northeast Fisheries Science Center
NOAA	National Oceanography and Atmospheric Administration
ONR	Office of Naval Research
RTK	Real Time Kinematic
PORTS	Physical Oceanographic Real-Time System
UHDAS	University of Hawaii Data Acquisition System
USGS	U.S. Geological Survey
UTC	Universal Time-Coordinated
WHOI	Wood Hole Oceanographic Institute

THIS PAGE INTENTIONALLY LEFT BLANK

ACKNOWLEDGMENTS

I would like to thank my advisor, Prof. Thomas Herbers, for his continuous guidance, clarity of judgment and focused approach throughout the preparation of thesis. I'm also grateful to Associate Prof. James MacMahan for his comments to further refine my thoughts. I am also thankful to Mr. Mike Cook, Mr. Paul Jesson and Mr. Chenwu Fen for their guidance and help in finalizing Matlab programming work. This project could not have been done without the dedication and participation of all.

I'd like to express my thankfulness to my family and friends who have supported and encouraged me throughout the years.

Finally, I humbly pay my thanks to Almighty who gave me untiring strength, guidance and wisdom, which resulted in successful completion of the thesis.

THIS PAGE INTENTIONALLY LEFT BLANK

I. INTRODUCTION

A. MOTIVATION AND BACKGROUND

The coastal environment affects nearly all aspects of human life, and its economic, social, political and strategic impacts on nations and people cannot be over emphasized. One of the important areas of coastal research is the knowledge of currents. Successful accomplishment of activities as diverse as navigation, maritime transportation, energy generation, naval military operations, search and rescue, oil spill response, recreational sports, and construction of piers, breakwaters and other coastal structures all depend to some degree on reliable information about currents in the relevant areas.

In addition, strength and orientation of currents shape the bathymetry, coastal features and sediment transport patterns. These currents are a combination of tidal and non-tidal components. Non-tidal components mainly include wind driven and density driven currents. Their relative contributions differ significantly from area to area and are sensitive to geographic features such as semi enclosed basins, bays and estuaries. In inlets, the tidal component is generally dominant and the currents have complex spatial (both horizontal and vertical) and temporal variations as a function of related geography, bathymetry and current generating forces.

This study focuses on the currents in the Golden Gate (Figure 1), the narrow entrance to San Francisco Bay. It is one of the most dramatic and dynamic coastal environments in the world (Barnard, 2005). It is a geographically constrained channel that acts as a tidal inlet for a large bay. Hence, tidal currents dominate the flow through the Golden Gate. Although tide generating forces are periodic in nature, the contribution of many constituents complicates the variability of sea level and currents. In addition to daily movements of a large volume of water through the Golden Gate, rivers also discharge fresh water in the bay and subsequent ocean. The bathymetry of the area is highly irregular with a large ebb tidal shoal offshore of the entrance that complicates the circulation dynamics. All these factors contribute to the temporal and spatial complexity of currents in this area.



Figure 1. San Francisco Bay and region of interest in Red rectangle (From Trump, 2008)

High resolution measurements of the spatial (vertical and horizontal) and temporal structure of current in inlets like the Golden Gate requires a large array of instruments that is usually not available. In such scenarios, ship mounted Acoustic Doppler Current Profilers (ADCPs) have shown their effectiveness in providing reliable data sets that complement sparse in-situ (Eulerian) observations. Present day automated systems enable logging of ADCP data without any additional costs, even when mobile platforms are involved in other operations. Processing of this type of data of opportunity can assist in better understanding of the current regime in an area of interest. This study uses ADCP data collected on several cruises when the R/V Point Sur was deploying various instruments in the Golden Gate as part of the Office of Naval Research (ONR) Coastal Inlets and River Mouths research initiative. The data was collected using a ship hull-mounted Teledyne RDI WH300 BroadBand ADCP.

B. RESEARCH QUESTIONS

1. Primary Research Question

Based on the ADCP recorded currents, what is the vertical structure of tidal currents in the Golden Gate channel and over the adjacent shelf and ebb tidal shoal?

2. Subsidiary Research Questions

How can ADCP profile transects be extracted automatically from an irregularly sampled ADCP data set?

Is it possible to infer the dominant temporal variations of the current structure (e.g., ebb vs. flood stages) based on the available irregularly sampled ADCP data set?

C. CONTRIBUTIONS

Official predicted currents for the Golden Gate Bridge area are available from NOAA which show the times of slack and strength of ebb/flood currents. These tables usually show surface currents and are produced based on astronomical factors only. The processing of available ADCP data in the area can contribute to a better understanding of tidal current regime in the Golden Gate, in particular:

- Understanding of vertical structure of tidal currents in inlets
- Knowledge of temporal variation of the vertical current regime
- Assist in planning of future ADCP observation if required
- Characterization of tidal currents in the Golden Gate for the ONR Tidal Inlets and River Mouths research initiative.

D. THESIS ORGANIZATION

Chapter II provides background information of currents and their relevance with respect to San Francisco Bay in general and the Golden Gate specifically. The ADCP measurement principle and important features relevant to the study are also discussed. Chapter III presents the field data, the methodology used for the automatic extraction of transects and the data processing procedures. ADCP transects of currents through the Golden Gate are presented and discussed in Chapter IV. Chapter V summarizes the results and offers recommendation for future research.

THIS PAGE INTENTIONALLY LEFT BLANK

II. BACKGROUND

A. SHALLOW WATER CURRENTS

Among, several mechanisms driving currents, tides, winds, and horizontal density gradients are the principal ones. Once a current is generated, various influences act to modify that current. The magnitude of these driving mechanisms and effects varies in deep and shallow waters due to significant differences in the area features and associated dynamics. In shallow waters, frictional and bathymetric effects exert strong influence and tidal forcing is often the dominant driving mechanism. Presence of continuous and excessive freshwater runoff may create density stratification. Moreover, coastal weather patterns also effect local forcing mechanisms. The combination of these factors results in high variability of coastal currents both in time and space.

1. Tides and Tide-Driven Currents

Gravitational attraction of the sun and moon to the Earth during orbital motions of the moon around the Earth and the Earth around the sun results in horizontal tractive forces in the ocean basins capable of generating tides. The primary frequencies of the tidal oscillations are clustered around the diurnal (24 h) and semidiurnal (12 h) period (Darwin, 1962). Constituent partial tides become in-phase and out-of-phase relative to each other, thus creating spring and neap tides on fortnightly and monthly time scales. During the spring tides, the partial tides reinforce each other such that the tidal range is relatively large and the tidal currents are more intense. During neap periods the partial tides cancel each other reducing the tidal level range and the strength of associated tidal currents (Walters, Cheng, & Conomos, 1985).

Tidal tractive forces create horizontal movement of water (tidal currents) to affect change in water level. Tidal currents are periodic in nature but there is a continuous variation in its amplitude. This variation is the result of the presence of three sub variations each of which is related to a particular movement of the moon. These movements are continuous changing of moon's phase, distance from the earth and declination with respect to earth in a cycle of 29.5, 27.5 and 27.5 days, respectively

(NOAA, 1981). Tidal currents exhibit changes in the strength that correspond closely with the changes in range exhibited by tides. Change in the moon's phase and distance results in proportional change of both tide and tidal currents whereas, change in tidal current is roughly half of tide change due to change in declination (L.P. Disney & Overshiner, 1925). The contribution of each variation towards varying tidal current differs with location to location. In general, current speeds peak during spring tides and reach a minimum during neap tides.

2. Non-Tidal Currents

Wind and density driven currents are the main constituents of non-tidal currents. Alongshore winds drive currents flowing along the coast in geostrophic balance. The current speed is generally maximum at the surface and gradually diminishes towards the seabed due to friction. River (freshwater) runoff and evaporation are major processes that lead to varying horizontal distribution of salinity or temperature in coastal regions, causing density driven baroclinic currents.

3. Time Scales of Tide, Wind and Density Driven Currents

Time scales of tide, wind and density driven currents is shown in Figure 2. Tide and wind-driven currents operate roughly over a similar range of time scales, whereas depending on the forcing mechanism, density driven currents operate across many time scales. At short time scales, ebb tides can extract fresh water from rivers to estuaries and then out to the sea leading to strong stratification in coastal regions. Heavy rains can result in excessive fresh water which may last for a day to few days.

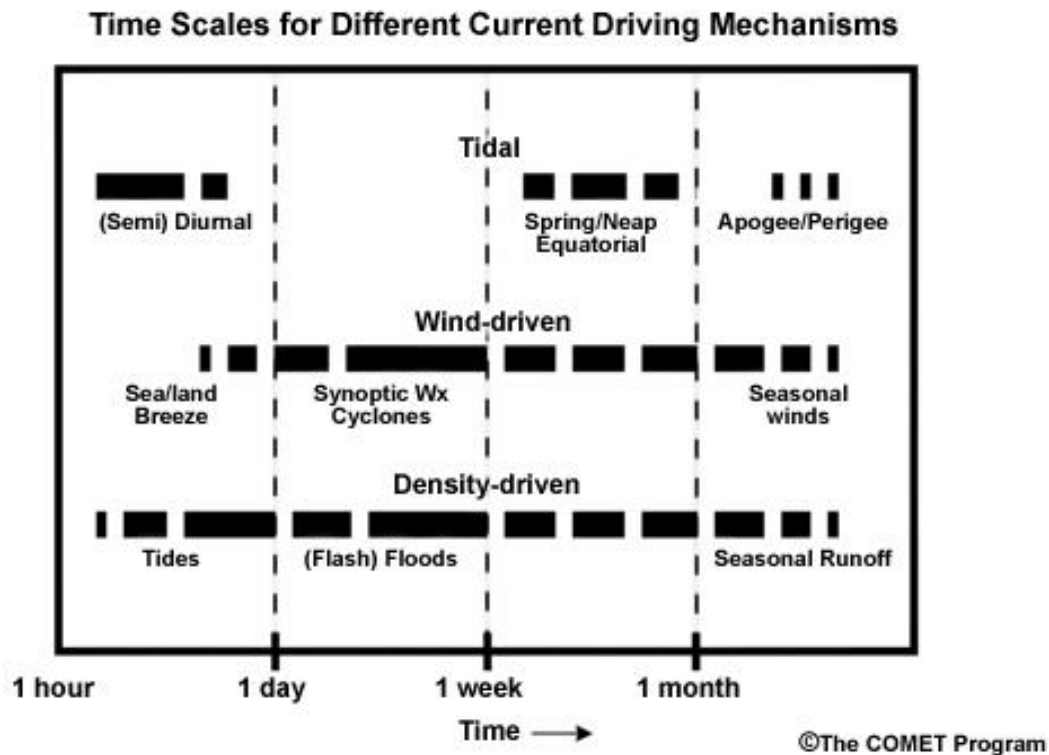


Figure 2. Time scales of different current driving mechanisms (From MetEd COMET Program)

B. SAN FRANCISCO BAY AND GOLDEN GATE AREA

1. San Francisco Bay

The Golden Gate is the only opening through which water inside the San Francisco bay interacts with the Pacific Ocean and vice versa. San Francisco Bay is a broad, shallow estuary comprising two geographically and hydrologically distinct sub-estuaries: the northern reach that lies between Golden Gate and the confluence of the Sacramento-San Joaquin River system in Suisun Bay, and the South Bay between the Golden Gate and the southern terminus of the bay (see Figure 3). The Sacramento-San Joaquin basin introduces about $600 \text{ m}^3/\text{s}$ (mean annual flow), with highest inflows during winter. Therefore, the northern part is a partially mixed estuary dominated by seasonally varying river inflow, and the South Bay is a tidally oscillating lagoon-type estuary (Conomos, Smith, & Gartner, 1985).

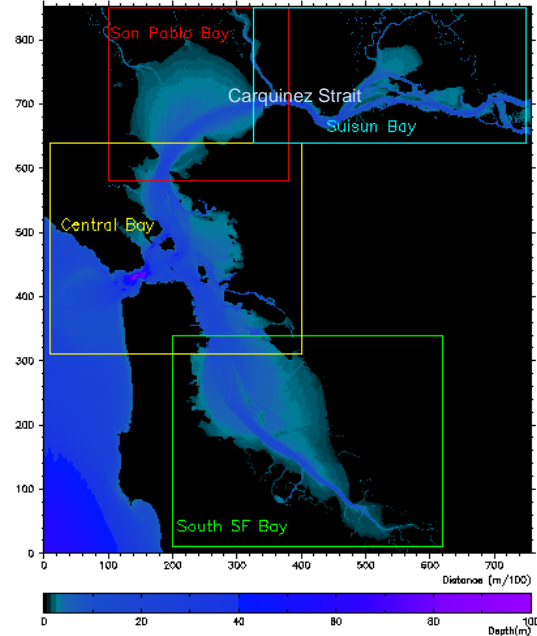


Figure 3. Geography of San Francisco Bay (From Grove, 2001)

The bay covers somewhere between 1,040 to 1240 square kilometers, depending upon inclusion of various mudflats (Conomos et al., 1985). The main part of the Bay measures 5 to 20 km wide in east/west direction and around 77 to 97 km in length in north/south orientation (Wikipedia, n.d. San Francisco Bay). The width of the Golden Gate is about 1.6 Km.

The average depth of the bay at MLLW is 6 m and it is characterized by broad shallows patches (2 m deep at MLLW) along with narrow channels that are typically 10–20 m deep. The deepest areas are Golden Gate (110 m) and Carquinez Strait (27 m) (see Figure 3) and being topographic constrictions, their depths are maintained by strong tidal currents (Conomos et al., 1985).

2. Bathymetric Features of Golden Gate and Offshore Area

Bathymetry of the area shows the deepest portion beneath Golden Gate, shoaling offshore to large ebb-tidal delta (the bar) covering over 100 km² that is fed by sediment flushed out of San Francisco Bay, and shaped by strong tidal currents associated with the Bay and waves originating from all sides of the Pacific (Barnard, 2005). A deeper shipping channel cuts through the middle of the bar (Figure 4).



Figure 4. Bathymetry of Golden Gate and adjacent offshore area (From Barnard, 2005)

Deeper depths underneath the Golden Gate are due to the strong tidal currents which have scoured the channel bottom into bedrock. As the strong ebb tidal jet spreads out and velocities decrease west of the Golden Gate inlet, the scouring potential sharply decreases, the coarse sediment load is dropped, and depths steadily decrease to 30 m over 2.5 km. This combination of factors has resulted in the formation of one of the largest sand wave fields (Barnard, 2005) (Figure 5). This field covers an area of approximately 4 km² in water depths ranging from 30 to 106 meters. At least 40 distinct sand waves with crests aligned approximately perpendicular to the tidally generated cross-shore currents can be observed (Barnard, Hanes, Rubin, & Kvitek, 2006). Consecutive bathymetric surveys conducted in 2005 determined that the average amplitude and wavelength of the 9 most western sand waves are 6.45 m and 79.58 m respectively (Wayman, 2005). The sand waves are expected to be important to the ebb and flood tidal currents at the entrance to San Francisco Bay because their effective roughness retards the flow, and eddies shed from flow separations near the crests thus causing substantial generation of turbulence (Barnard, Hanes, Rubin, & Kvitek, 2006).

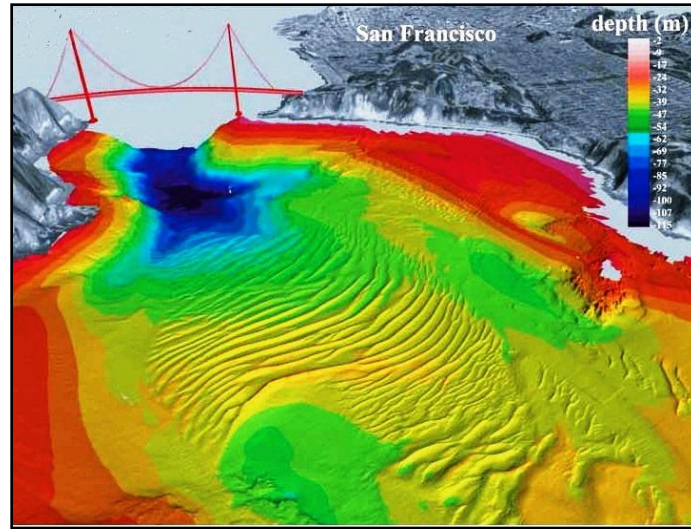


Figure 5. Oblique view of the giant sand waves and other bed forms at the mouth of San Francisco Bay (From Barnard, Hanes, Rubin, & Kvitek, 2006).

3. Tides and Tidal Currents

San Francisco Bay is protected from the strong wave action as it is isolated from the open ocean by land except at the Golden Gate. In such environments, tidal currents are constrained to flow along the channel axis and reverse rapidly after short periods of slack water.

The large spatial expanse of San Francisco Bay and tidal ranges of up to 1.7 m, translate into the movement of an enormous volume of water into and out of San Francisco Bay through the Golden Gate during each tidal cycle. This quantity, i.e tidal prism, is equal to nearly one-fourth of the bay's total volume (Grove, 1998,2001). As per another estimate, the Golden Gate spring tidal prism is $2 \times 10^9 \text{ m}^3$ that means 528 billion gallons every 6.1 hours during peak flows (Barnard, 2005). The freshwater discharge rate into the bay of $800 \text{ m}^3/\text{s}$ (211,000 gallons/sec), is less than 1% of the overall tidal flow (Barnard, 2005). As a result, strong ebb and flood tidal currents are observed twice each day at the Golden Gate, with depth-averaged tidal currents exceeding 2.5 meters per second during peak ebb flows (Barnard, Hanes, Rubin, & Kvitek, 2006).

a. Character of Tide and Tidal Currents

Oceanic tides propagate landward through Golden Gate as shallow water waves. The amplitudes and the phases of these incident tidal waves are modified by bathymetry, reflections of the waves from shores and bottom friction. The distinction between standing and progressive waves is important for understanding major features of the tides and tidal currents in the bay. A progressive wave propagates down a long channel with wave crests moving forward at a certain phase speed. For tidal waves (shallow-water waves), the phase speed depends only upon the depth and the crest advances horizontally. The times of high and low water progress from one end to the other. The horizontal current speed slacks closer to mid-tide and the strongest currents occurs near high/low tide. Standing waves typically occur in semi-enclosed basins where the wave is reflected back upon itself. The water surface oscillates vertically between fixed points i.e nodes without progression. Slack currents occur at high and low waters (Walters et al., 1985).

At the Golden Gate, the tidal wave behave as a mixture of a progressive and a standing wave. The northern reach is characterized by having a partial progressive and standing wave, whereas South Bay is characterized by having a standing wave (Walters et al., 1985).

In order to obtain the tidal character of tides in San Francisco, NOAA published amplitudes of 4 major harmonic constituents (O_1 , K_1 , M_2 and S_2) (NOAA). The amplitude ratio of the sum of diurnal to sum of semi-diurnal constituents is 0.83 which falls within the limits of mixed semi-diurnal tides (POLTIPS 3 Guide, n.d., Proudman Oceanographic Laboratory). It implies that two unequal high and low tides occur each 24.84-hr day, usually with large differences between successive high tides and successive low tides (Figure 6A). The difference of tidal levels in mixed tides vary considerably within a lunar month, from nearly equal tides to a maximum difference of over 1.5 m within a lunar day (Conomos et al., 1985). Variations between measured and predicted values of tidal height (Figure 6B) elaborated upon by Walters and his co-workers (Walters, 1982; Walters et al., 1985) are attributed to variations of winds and river discharge.

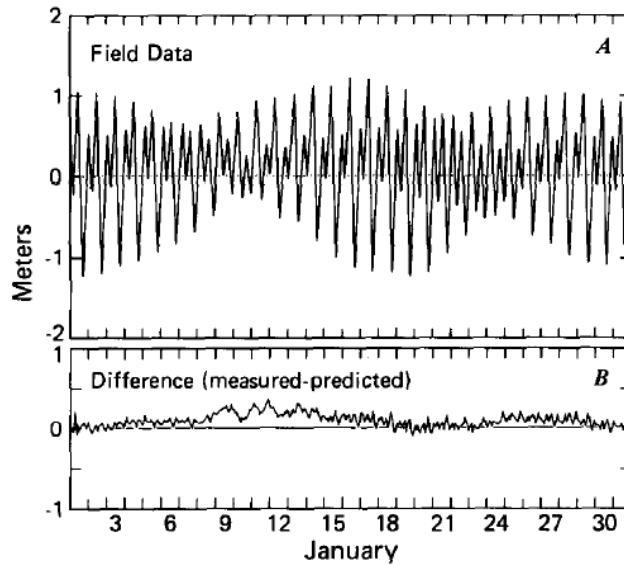


Figure 6. Tidal Data of San Francisco Bay (From Cheng & Gartner, 1984)

Based on 19 years i.e from 1983–2001 tide observations, values of important tidal datums w.r.t Mean Lower Low Water (MLLW) are given in Table 1.

Table 1. Important Tidal Datums-San Francisco (NOAA Datums-San Francisco)

Levels Above MLLW	Meters above/below MLLW
Mean Higher High Water (MHHW)	1.780
Mean Higher Water (MHW)	1.595
Mean Tidal Level (MTL)	0.970
Mean Low Water (MLW)	0.346

If the tidal current is not affected by wind or river run off, the flood and ebb current velocities, and the durations of flood and ebb will be approximately equal. Presence of non-tidal currents can significantly modify characteristics of the tidal current. As the flood current moves up estuaries and inlets, river flow starts to affect it. Depending on strength of inflow, it increases the ebb strength while decreasing the flood

strength. Also slack before flood gets delayed, while slack before ebb occurs earlier (NOAA, 1981). Hence, the duration of ebb and flood is increased and decreased respectively.

NOAA predicted and observed sea level and predicted currents at the Golden Gate, during a spring cycle, are shown in Figure 7. The Lower Low Water (LLW) follows the Higher High Water (HHW) resulting in usually stronger ebbing current than the flooding (Cheng & Gartner, 1984). On average, slack water occurs 2 hour after HW/LW indicating large departure from a pure standing wave that is likely caused by frictional effects in the large shallow estuary. The almost uniform time interval between slack waters is consistent with minimal effects of river discharge that contribute only about 1% of the total volume transported in one tidal cycle.

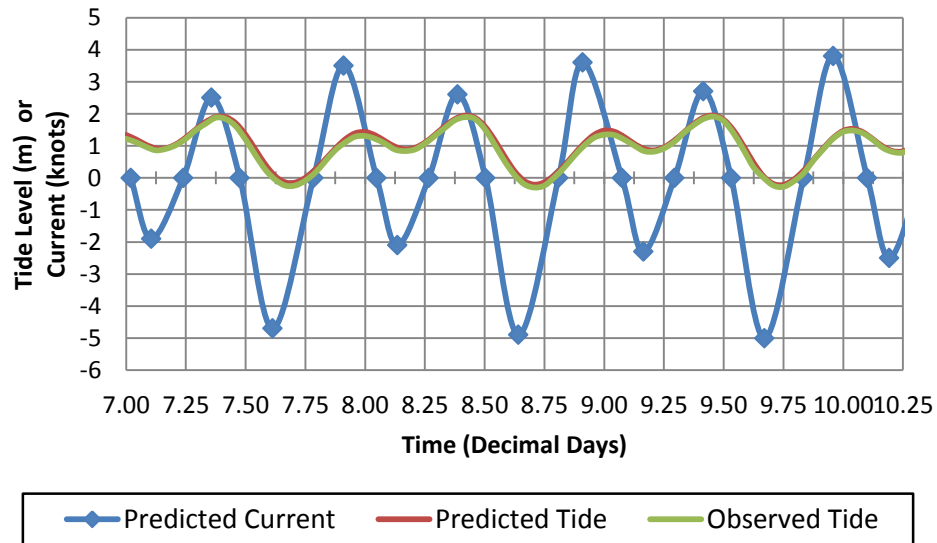


Figure 7. Comparison of sea level and current (7–10 January 2010) at Golden Gate (After NOAA Tides and Currents, 2012)

b. *Spatial Variability of Tidal Currents*

Bottom friction strongly affects the speed of the currents. The directions of the tidal currents are generally tangent to the basin isobaths, whereas the magnitudes of the tidal currents are proportional to the mean water. The inflow follows the depths along the south shore of the entrance to the bay, whereas the surface outflow tends to follow the

shoal areas and is concentrated toward the northern shore (Walters et al., 1985). With respect to vertical structure, the tidal current velocity generally decreases from the surface to the bottom, and near the bottom, velocities are estimated to about two thirds of that at the surface (NOAA, 1981).

4. Modeling of tidal currents of San Francisco Bay

NOAA installed Physical Oceanography Real-Time System (PORTS) in San Francisco Bay to provide now-casts of sea level, tidal currents, salinity, and meteorological conditions. The system takes meteorology and tide input from 5 shore stations and current input from 5 ADCPs at 6 minute interval. It uses a semi-implicit, finite-difference model known as Tidal, Residual, Intertidal Mudflat (TRIM) model (Cheng, Casulli, & Gartner, 1993). The model is executed every hour for a 48 hours simulation. A 200 m uniform finite-difference grid is used for San Francisco Bay, California (Cheng & Smith, 1998). The results are made available to users at near real-time on web. An example prediction shown in Figure 8, visualizes the flood current entering San Francisco Bay.

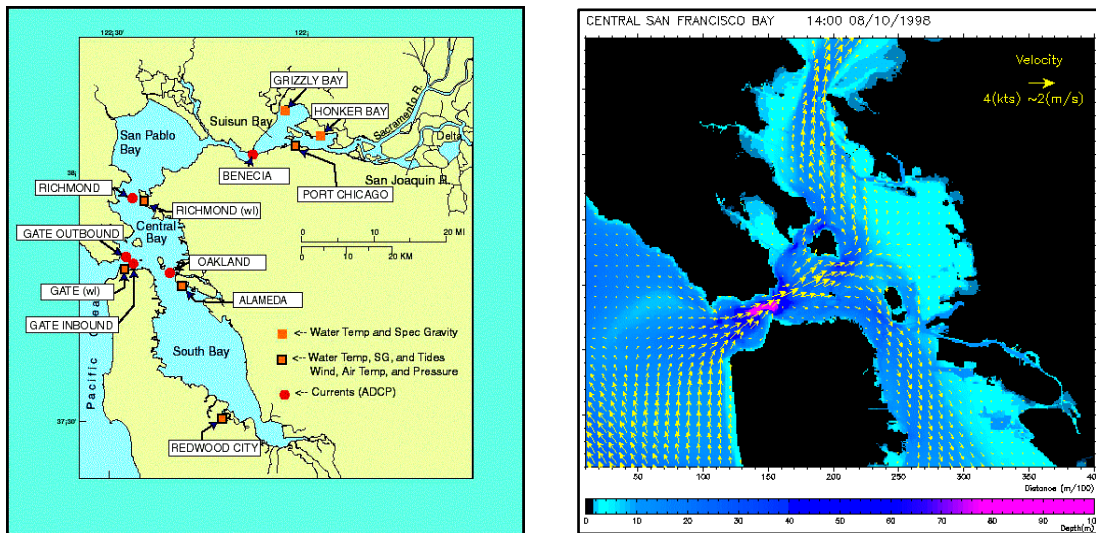


Figure 8. PORTS sensor locations map (left) and current product (right) (From Cheng & Smith, 1998)

C. MEASUREMENT OF CURRENTS

A variety of current measurement techniques exist, each with their own limitations and advantages. Drifters are mainly used for Lagrangian measurements of surface currents. Shore-based High Frequency (HF) radars can provide spatial coverage of near surface currents with a typical horizontal resolution of 1 km (Matthews, Simpson, & Brown, 1988) and a range of 20 km. This method has been used successfully to measure horizontal current structure in energetic coastal flows (Holbrook & Frisch, 1981; Matthews, Simpson, & Brown, 1988; Prandle, 1987). Recent advances in satellite-based Synthetic Aperture Radar (SAR) observations also have the potential to measure surface currents and preliminary comparisons between HF radar and SAR current measurements appear promising (Danilo, Chapron, Mouche, Garello, & Collard, 2007).

For Eulerian measurements, moored current meters are used traditionally. They may work on mechanical or electromagnetic principles and can be deployed at various vertical separations and depths. Moored measurements provide excellent resolution of temporal variations in currents but are not well suited for determination of spatial structure, which favors continuous, rather than discrete sampling in space (Geyer & Signell, 1990).

The most widely used instrument for measuring currents is the Acoustic Doppler Current profiler (ADCP). The instrument can be mounted horizontally on seawalls or bridge pilings in rivers and canals to measure the current profile from shore to shore. In very deep areas, they can be lowered on a cable from the surface (Physical Oceanography Department-WHOI, n.d). In shallow waters, it can be deployed on the seabed that enables recording of long time series of vertical structure of currents at a particular location. When mounted on the hull of ships, it can be used in a survey mode to collect transects of velocity profiles. Shipboard ADCPs have been used to measure spatial variations in currents in the deep ocean (Regier, 1982) and on the continental shelf (Kosro, 1985; Barth & Brink, 1987). In these applications the ship's navigation system was used to remove the ship's motion from the measured ADCP velocities.

Detailed information on operating ADCPs can be found on the websites of leading ADCP manufacturers like Teledyne RD Instruments (RDI) and Sontek. Since shipboard ADCP was used for the data collection of the study, a brief review of its working principle, processing, possible errors and limitations is given here.

1. ADCP Basic Principle

The ADCP works on the principle of the Doppler shift of sound effect and uses acoustic transmitters. It may have two to five transducers that also act as receivers of the backscattered pulses (Gunawan & Neary, 2011). It precisely measures the change in the frequency between the transmitted ping and the acoustic energy reflected back from suspended particles in the water column. Sound waves bounced back from a particle moving away from the profiler have a slightly lowered frequency when they return whereas particles moving toward the instrument send back higher frequency sound.

To observe velocities at different depth levels, the ADCP uses a range gating process that breaks up the returned signal into shorter segments. Each segment contains the return from a sample volume at a distance equal to half the distance travelled by sound waves during the elapsed time interval.

Shipboard ADCPs are provided with the precise positioning using DGPS or RTK and ship's heading. This information is used to convert the velocity components into earth and ship based coordinates. The first generations of ADCPs, often called 'narrow band' utilized a single pulse in each ping for each velocity measurement. In the early 1990s the broadband ADCP was introduced in which each ping consists of multiple short pulses (Gunawan & Neary, 2011). Hence, BroadBand ADCP provides more independent samples within a single pulse and significantly lower standard deviation in measured velocities (Griffiths, 2004). In this study an RDI WH300 Broadband ADCP was used.

Broad band processing works in the time domain instead of frequency. Movement of particles towards or away from the transducer results in change in the relative phase which is easier to measure than change in frequency. However, this might create ambiguity regarding total number of full cycles. This 'ambiguity' is resolved by sending coded pulses all inside a single long pulse and then using 'autocorrelation' technique to

regroup the returns (Teledyne RD Instruments, 1996). For best results in different conditions, different modes with different time lags and pulse forms are used (NEFSC-NOAA, 2006).

The ADCP uses multiple beams pointed in different directions for sensing different velocity components. One beam is required for each current component. Therefore, to measure three velocity components (e.g., east, north, and up), the ADCP must have at least three beams. If the ADCP beams point in other directions, trigonometric relations can convert current speed into north and east components. (Teledyne RD Instruments, 1996).

RDI Broadband ADCPs use four beams pointing at an angle of 20° in convex configuration and assume that currents are horizontally homogeneous. First pair of beams obtains East-West horizontal component and a vertical velocity component whereas the second pair measures North-South horizontal component and another vertical velocity component (see Figure 7).

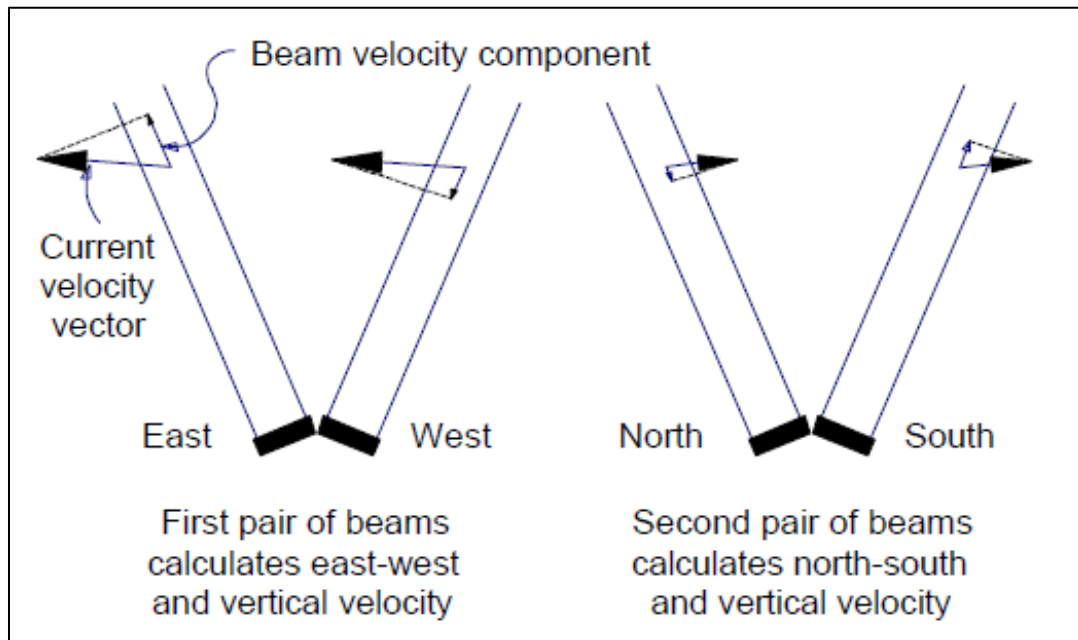


Figure 9. The relationship of beam and earth velocity components (From Teledyne RD Instruments, 1996)

The difference between the two estimates of vertical velocity obtained from two pairs of beams is the error velocity. Error velocity allows validation of the assumption of horizontal homogeneity over the distance separating the beams. It also enhances redundancy, that is if one beam provides bad data, all 3 velocity components can still be estimated.

The four beam ADCP transducer configuration is called the Janus configuration (see Figure 9) which is good for rejecting errors in horizontal velocity caused by tilting (pitch and roll) of the ADCP. The two opposing beams allow cancellation of vertical velocity to yield unbiased estimates of horizontal velocity. Errors introduced by the pitch and roll are reduced in the Janus configuration to second order; that is, velocity errors are proportional to the square of the pitch and roll errors.

The RDI ADCPs with bottom tracking feature can measure the velocity of the instrument relative to the water (known as water tracking), as well as the velocity of the instrument relative to the bottom (known as bottom tracking). Experiments have shown that bottom tracking is excellent at measuring a boat's speed. The net boat displacements measured by bottom tracking are comparable in accuracy to those measured by a RTK GPS (Fong & Monismith, 2004).

Errors in the ship's gyrocompass can contaminate ADCP speed estimates. The RDI Workhorse ADCPs, contain their own compass that monitors pitch, roll, and heading of the instrument. By being self-contained, problems related to the ship's gyrocompass are removed along with issues related to the orientation of the instrument with respect to the vessel (Fong & Monismith, 2004).

Standard profile data of BroadBand ADCP mainly includes velocity data, correlation, echo intensity and percent good data. Although, earth coordinates of velocity are normally used but velocity data can be acquired in user selected format and coordinate system (beam, earth, ADCP or ship). Echo intensity shows receiver's received signal strength whereas correlation is a measure of data quality in scaled units such that the expected correlation is 128 if high signal/noise ratio exists. Percent good data

indicates what fraction of data passed a variety of criteria. Rejection criteria includes low correlation, large error velocity and fish detection. Default thresholds differ for each ADCP.

2. Accuracy and Limitations of ADCP Measurements

The current generation of RDI BroadBand ADCPs transmits the pulse filled with a wide band code consisting of alternating phase reversals of the carrier frequency. This results in many independent measurements of the velocity during the averaging interval of a bin. This considerably improves the precision of the velocity measurement (Fong & Monismith, 2004).

ADCP single-ping velocity has large errors among which the most noticeable are the short term random error and long term bias. The single-ping random error can range from a few mm/s to as much as 0.5 m/s. The size of this error depends on internal factors such as ADCP frequency, depth, cell size, number of pings averaged together and beam geometry. External factors include turbulence, internal waves and ADCP motion. Bias is typically less than 10 mm/s (Teledyne RD Instruments, 1996) but the exact sources of error contributing to the bias are unknown.

The total error size in ADCP single-ping velocity is too large to meet most measurement requirements. Therefore, single ping data is averaged to reduce the measurement uncertainty to acceptable levels. As random error is uncorrelated from ping to ping, averaging reduces the standard deviation of the velocity error by the square root of the number of pings (Teledyne RD Instruments, 1996). After averaging for a certain period of time, the random error becomes smaller than the instrument bias and further averaging will do little to reduce the overall error.

An important limitation of ADCP performance is its dependence on the presence of particles in the water column. In very clear waters the pings may not hit enough particles to produce reliable data. Another limitation is generation of bubbles below the ocean surface due to breaking waves. When bubbles pass under the ship's hull, they can act as a shield that reduces the ADCP profiling range and, in the worst case, completely blocks the sound transmission (Gunawan & Neary, 2011). Also, the choice of frequency

involves a tradeoff between range and precision. High frequency pings yield more precise data but low frequency pings have longer ranges.

3. Applications of Shipboard ADCP Data Collection

ADCPs have been used to characterize the current structure of both the deep and near-surface currents of the world's oceans (King, Firing, & Joyce, 2001) as well as flows in estuaries. The depth-averaged currents measured from shipboard ADCP are also being used for comparison with tidal currents obtained from two-dimensional numerical models (Howarth & Proctor, 1992). In estuarine hydrodynamics, ADCPs have made possible new conceptual models of estuarine circulation (Geyer, Trowbridge, & Bowen, The dynamics of a partially mixed estuary, 2000). Improvement in ADCP technology has also enabled the measurement of stratified turbulence (Stacey, Monismith, & Burau, 1999) and directional wave spectra (Terray, Gordon, & Brumley, 1997). ADCPs are also being utilized in the selection of sites for electricity generation based on the detailed characterization of currents at a site (Epler, Polagye, & Thomson, 2010).

With respect to physical oceanography, two main techniques have been used to resolve the structure of currents using shipboard ADCP. One includes the repetition of transects in a regular pattern to carry out harmonic analysis that resolves tidal current constituents. This approach was used to map the currents through the Minch between Scotland and Herbides (Simpson, Mitchelson-Jacob, & A. E. Hill, 1990) and around a headland in Vineyard sound, Massachusetts was carried out in 1988 (Geyer & Signell, 1990). A second method to resolve the spatial resolution of tidal currents from shipboard surveys was tested in the Yellow sea (Candela, Beardsley, & Limeburner, 1990). This method uses a least-square analysis to fit amplitudes and phases of the M_2 and K_1 tidal constituents as functions of spatial position to the data.

III. DATA AND METHODOLOGY

A. DATA COLLECTION AND PROCESSING ONBOARD SHIP

1. ADCP Arrangement on Ship

ADCP data were collected using an RDI ADCP WH 300 that operates at 300 KHz and ping rate of 2 Hz. The number of depth cells can range from 1–128. Decrease in the size of depth cell decreases the range and increases the single-ping standard deviation. For the 2 m depth cell size used here, the typical range is 78–102 m with 6.1 cm/s single-ping standard deviation. Ensemble averaging of single pings considerably reduces the standard deviation. More detail of the WH 300 is available at the following link:

http://marineops.mlml.calstate.edu/sites/default/files/wh_mariner_ds_lr.pdf

The RDI WH 300 is mounted in the hull of the R/V Point Sur directly at mid-ships. The unit is recessed into a void so that it does not protrude past the contour of the ship's hull. This arrangement reduces the bubble formation in vicinity and hence enhances its performance. Typically, for a system like the WH 300, 2 m blanking range is considered (Gunawan & Neary, 2011). Blanking range is the distance of the first bin from the transducer that can be measured by the ADCP. The inability to measure within this range is due to the time overlap between transmission and reception of sound pulses in the region adjacent to the ADCP transducer. Draught of the ship and blanking range results in logging the first velocity measurement at 7.07 m below the mean sea surface.

2. Overview of Data Collection and Onboard Processing

University of Hawaii Data Acquisition System (UHDAS) refers to a suite of programs and processes developed at the University of Hawaii that performs data acquisition, data processing, and monitoring at sea. This provides as close to a final dataset as is reasonably automatable while maintaining the to reprocess the data from scratch if necessary. A brief overview of the system is given below, but its full documentation can be found at the following link:

<http://currents.soest.hawaii.edu>

The data acquisition component of UHDAS enables setting ADCP parameters, start pinging, collection of binary records from ADCP ensemble and collection/time stamping of ancillary data (position and heading). All data is recorded in Universal Time-Coordinated (UTC) zero-based decimal day format. UHDAS also provides data access via the ship's web and shared network drive.

At sea, a UHDAS installation uses CODAS processing to calculate ocean velocities from ADCP measured velocities, position, and heading. Thereafter, in the CODAS Post-processing step, correction of gyro heading, application of scale factor and editing out of bad bins and profiles is automatically conducted. The final processed output is written as Matlab files and NetCDF files. Detailed information of processing is available at the following link:

http://currents.soest.hawaii.edu/docs/adcp_doc/codas_doc/index.html

3. Detail of Collected Data

The analyzed data comprises four data sets of the research cruises undertaken onboard the R/V Point Sur. These cruises were conducted from 11 to 13 October 2011, 14 to 16 February, 26 to 28 April, and 17 to 18 October, 2012. The track of the ship while collecting data in vicinity of the area of interest is shown in Figure 10.

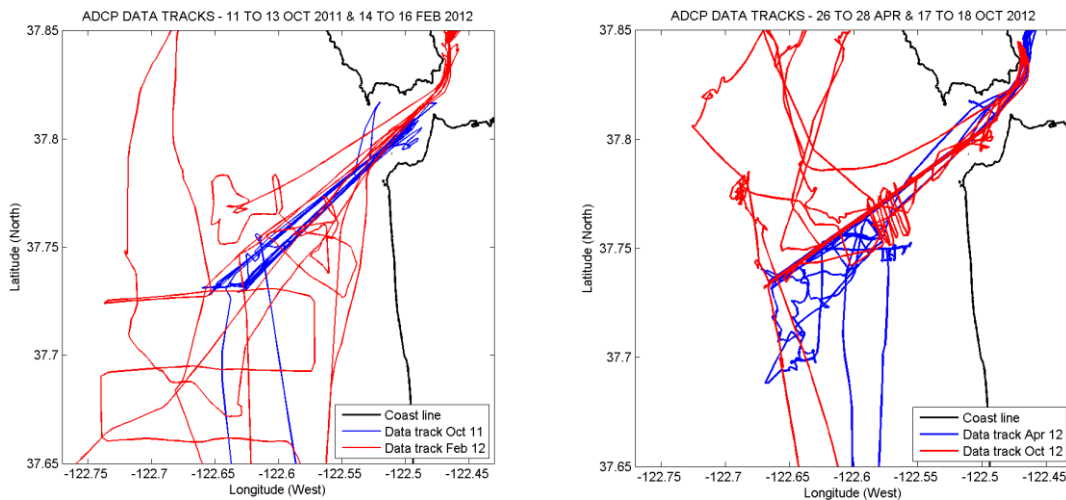


Figure 10. Ship tracks during ADCP data collection

All the data collected in 2012 has a temporal interval of 2 minutes and depth cell size i.e vertical separation of 2 m. This means if the ship moves at 7–8 Kts then on average, there is one averaged profile per 400–500 m. Data collected in October 2011 have 5 minutes interval with a cell size of 1 m thus enabling one averaged profile every 1200 m at 8 Kts speed. For each depth cell in a profile an average value of eastward (u), northward (v) and vertical (w) velocity component is recorded in units m/s. Additionally, for each depth cell, the values of error velocity, last good bin (lgb), and signal return amplitudes of each beam are recorded. This data helps in final editing/ post processing. Time (decimal day format) and position (Latitude and Longitude), associated with each profile is also recorded.

B. DATA PROCESSING METHODOLOGY

Figure 10 shows that the collected ADCP does not provide complete spatial coverage of the area of interest. Temporal coverage is also irregular. In this scenario, gridding the data spatially in horizontal bins and then analyzing each bin in the temporal domain will not bring out meaningful results. Instead, dividing the data into transects traversed in a particular direction for a reasonable time length is a better choice. As the temporal changes in tidal currents over the 1–2 hour sampling period of each transect is relatively small compared to the spatial variations, the transects can be roughly considered as displaying a snapshot section of the current.

1. Extraction of Transects

Manual extraction of transects is possible but it takes time and is too cumbersome while dealing with dense or overlapping data. In addition, with recurrent cruises in the same area the process is required to be conducted manually for each cruise. Therefore, a Matlab code that is able to automatically extract transects will save both time and effort while dealing with multiple data sets. Introduction of interactive input features will make it generic and enable its application to variety of ADCP data collected in different geographic areas.

Initial analysis of the ADCP tracks highlights a few difficulties towards automated extraction of transects. There is a lot of spatial overlapping and crossing of

tracks which make it impossible to pick transects based on geographic parameters. Moreover, as data tracks exhibits varying lengths of tracks, building a code based on time will not be feasible. Sometimes the ship's heading is changing abruptly during a change of course whereas in other cases the rate of change of heading is slow when she is adjusting a course to avoid shallow coastal features like turning northward while moving inshore of the Golden Gate Bridge. Similarly, during a transect, sometimes the ship is stopped or moving slowly to conduct a CTD cast or recover a drifter. Rates of change of speed and heading can be quantified. Therefore, an automated code using a combination of geographic criteria and the rates of change of heading and speed is needed. As different values of these parameters are required to handle different data sets, the code has to be interactive.

a. Overview of the Transect Extraction Methodology

Generally, the logged data are continuous and connected to the time base right from the start to the end of the cruise. Therefore, as a first step the data within the desired area is selected that is continuous in time. Thereafter, the data are broken down to different segments which can be termed as basic transects. This is achieved by terminating transects when the ship changes speed or direction. Ship's speeds and headings are calculated using successive positions logged at the 2 or 5 minute interval between profiles. A large decrease in ship's speed may indicate the ship has stopped and similarly a change in heading may indicate the start of new transect. The primary criteria used here are the maximum allowed changes in ship's heading and speed between two successive profiles.

Additional parameters of maximum and minimum ship speeds further refine the transect selection process. Setting a maximum allowed speed avoids sparsely sampled transects while a minimum speed threshold eliminates data when ship was holding a station.

Transects selected based on the above parameters can be of varying lengths and orientations. The automated selection of final transects takes into account two additional filters. These include minimum length (number of data points) of transect and

a heading filter. A minimum length filter rejects transects of short lengths. A heading filter with a combination of minimum and maximum true and reciprocal headings allows selection of transects only in some particular orientation (for example aligned with the Golden Gate channel).

b. Overview of the Matlab Processing

First, the required data are extracted from the ADCP database structure. This includes time, position, current velocities and quality parameters like last good bin, amplitudes and percent good. Last good bin indicates farthest/deepest bin number within a profile that has good quality data. To reject velocity data below ‘lgb’, velocity and depth data below ‘lgb’ are changed to NaN. This is an option which can be ignored if all data is required for manual editing. The code also provides an option of using a polygon (mouse entered) for selecting data within an area of interest. This can significantly reduce the amount of data to be handled. Next, statistical information on speed and heading, including maxima, minima, average values and histograms are computed (see Figure 11).

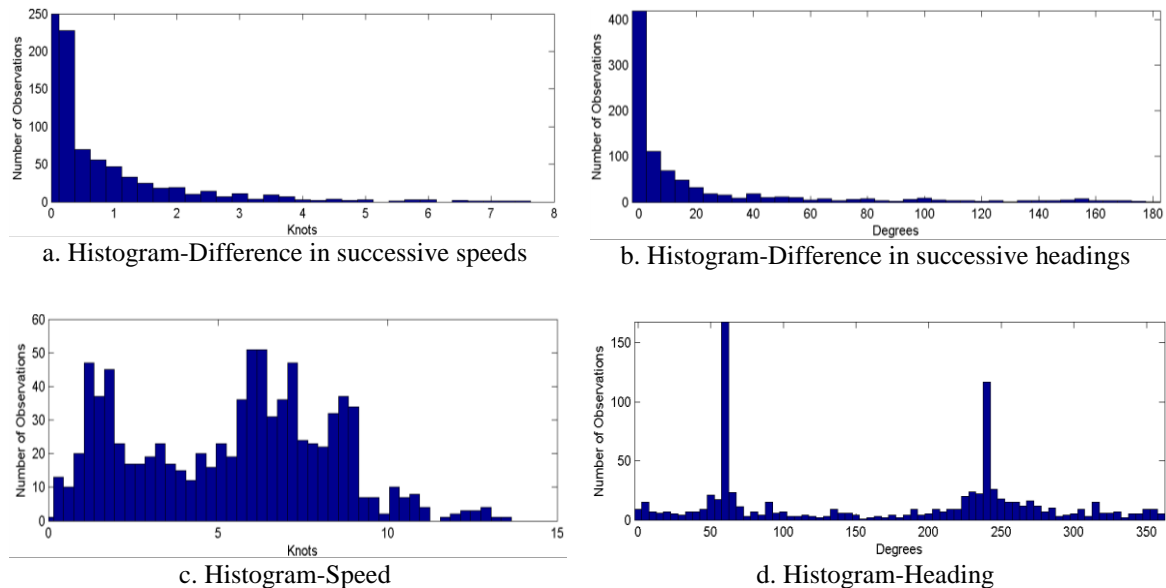


Figure 11. Example histograms of Speed and Headings

Statistical information assist in determination of probable limits of variables to be used in extraction of transects. Histograms of speed and heading (see Figure 11-a and b) indicate that speed is ranging from 0 to 13 Kts and there are two headings, where most of the data is collected. Similarly, (see Figure 11-c and d) for most of data, difference of speed and heading between successive profiles is within 3 Kts and 20 degrees, respectively. The code also generates histograms with smaller horizontal intervals to provide more detailed information for quick determination of balanced limits of variables for transect extraction.

Finally, the transects that pass all criteria are plotted for visual inspection. If, the result is not satisfactory then the values of variables can be changed to get the desired result. The optional filters of minimum data length and heading can be used to further reduce the number of transects. The tracks of the finally selected transects of each data set are shown in Figure 12.

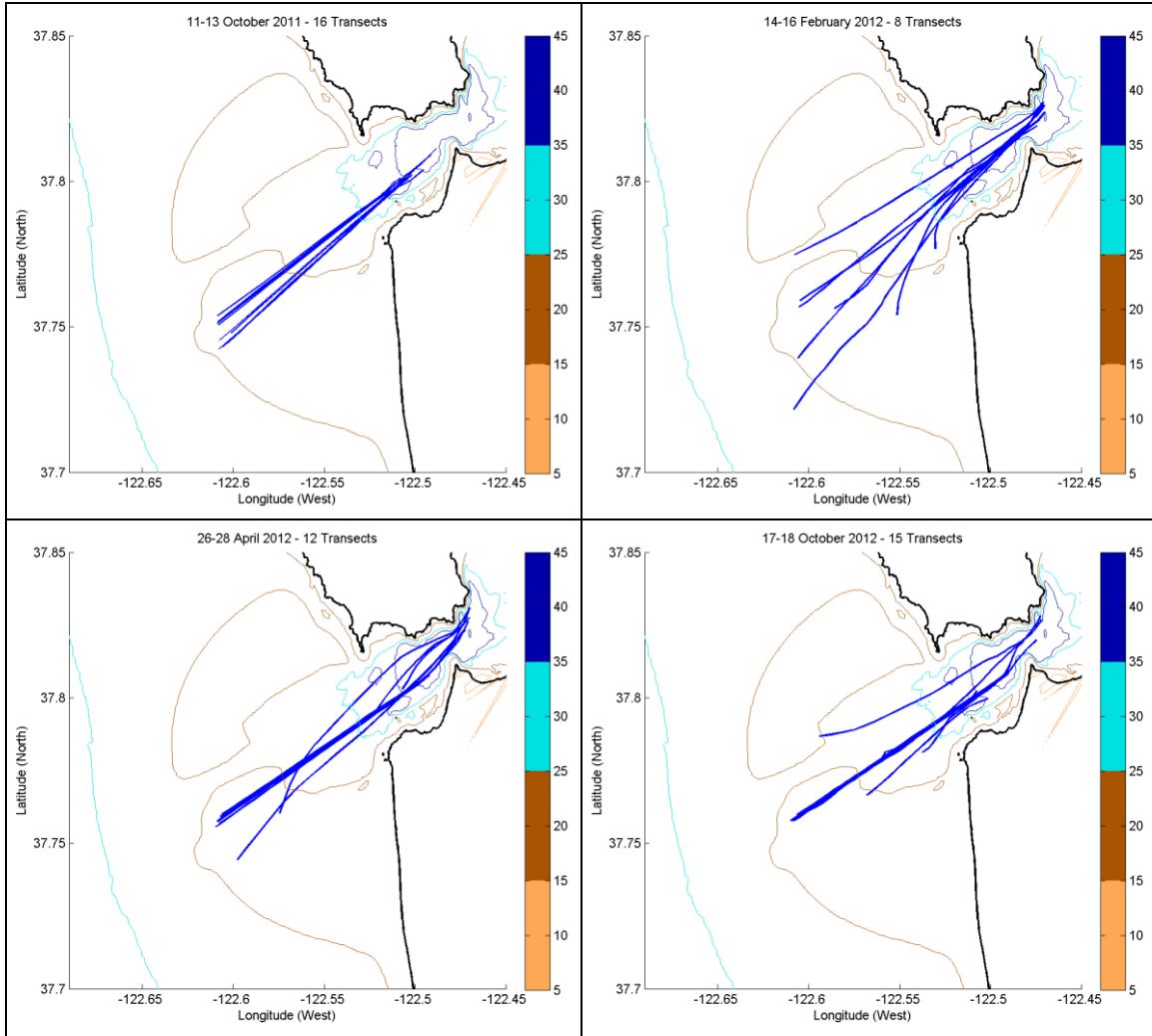


Figure 12. Geographical location of final extracted transects

2. Post Processing/Editing of Data

The WH 300 ADCP processing suit applies its own criteria for determination of 'lgb'. As a consistence of check, the depth of the deepest bin passing the 'lgb' criteria was compared with the nearest bathymetric data. Although, in most cases, the 'lgb' cutoffs are consistent with the independent depth estimates, sometimes bad data were able to pass through, as shown in Figure 13.

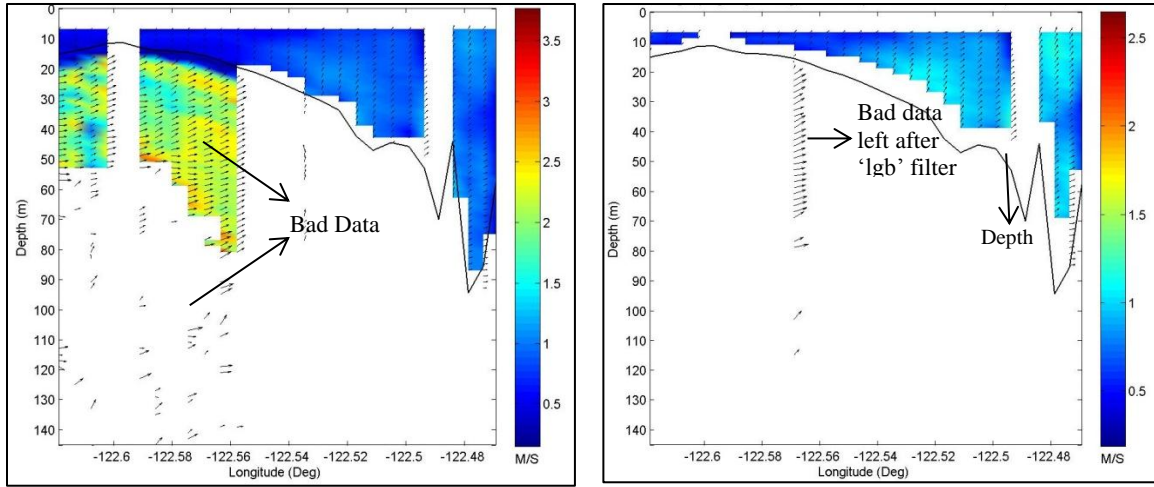


Figure 13. Current strength data before and after applying 'last good bin (lgb)' filter

Based on the overall effectiveness of the 'lgb' filter, a two-step methodology is adopted. At first, all current data below last good bin is replaced with NaN values. In the second step, any remaining data still encountered below the sea floor are also replaced with NaN values.

IV. RESULTS

The four data sets analyzed during the study were collected in different tidal conditions. Two (February and April 2012) data sets were collected during neaps or near neap conditions whereas the other two sets (October 2011 and October 2012) were gathered during springs. The post processed data of October 2011 showed irrecoverable errors in current velocity and hence is ignored for final presentation of current structure. Data from the three later cruises gathered and processed using the automated UHDAS system passed quality checks and showed consistency, and are presented here. On a few occasions, bad data were noted below the ‘last good bin’ determined by the system and removed. Temporal averaging of 2 minutes data proved adequate to resolve the larger scale horizontal current structure, although it may not capture small scales eddies near the bottom.

A large number of transects have been obtained from the three remaining data sets but only a few representative examples are discussed in this chapter. These include two cases each for flood and ebb current cycles with one presenting a low tidal range/current scenario and the other a high range situation. A separate case showing cross channel variation is also discussed.

Each scenario is represented by two to three plots of transects undertaken in inshore or offshore direction. Each plot shows average heading, start and end times on top and a line indicating the approximate seabed elevation is also plotted for reference and checking the suitability of ADCP data. The seabed profile along the transect was interpolated from gridded bathymetric data with 40 m spatial resolution. Direction of horizontal current is shown with arrow and strength is presented by its length in ‘quiver’ depiction. The plots are also superimposed with the pseudo colors showing the current strength in meters/second while leaving the upper 7.07 m (ship’s draught and ADCP blank range). Geographical positions of transects, predicted tide and tidal currents and legend of pseudo color is also shown with each case.

A. FLOOD CURRENT CASE

1. LOW RANGE FLOOD

The three transects from the low range flood case of April 2012 feature a tidal range of 0.52 m occurring over 5.5 hours. Transect 1, 2 and 3 (see Figure 14) followed nearly identical tracks along southern side of channel, traversed during the first/second, third/fourth and fourth/fifth hours of flood current, respectively.

Maximum flood current values agree with the predictions of NOAA (NOAA Tides and Currents, 2012). During the entire flood cycle, the current remains bottom intensified with significantly more strength in deeper areas than the shallower ones. Throughout the flood cycle bottom currents flow in the north-east direction, whereas near surface currents are directed between north and north-east except during peak flood time when its direction is mainly easterly.

With the temporal progression in the flood cycle, the current intensifies proportionally in the entire water column while remaining bottom intensified. Similarly, while maintaining bottom intensification, it decreases proportionally from near surface to bottom during the latter half of flood cycle.

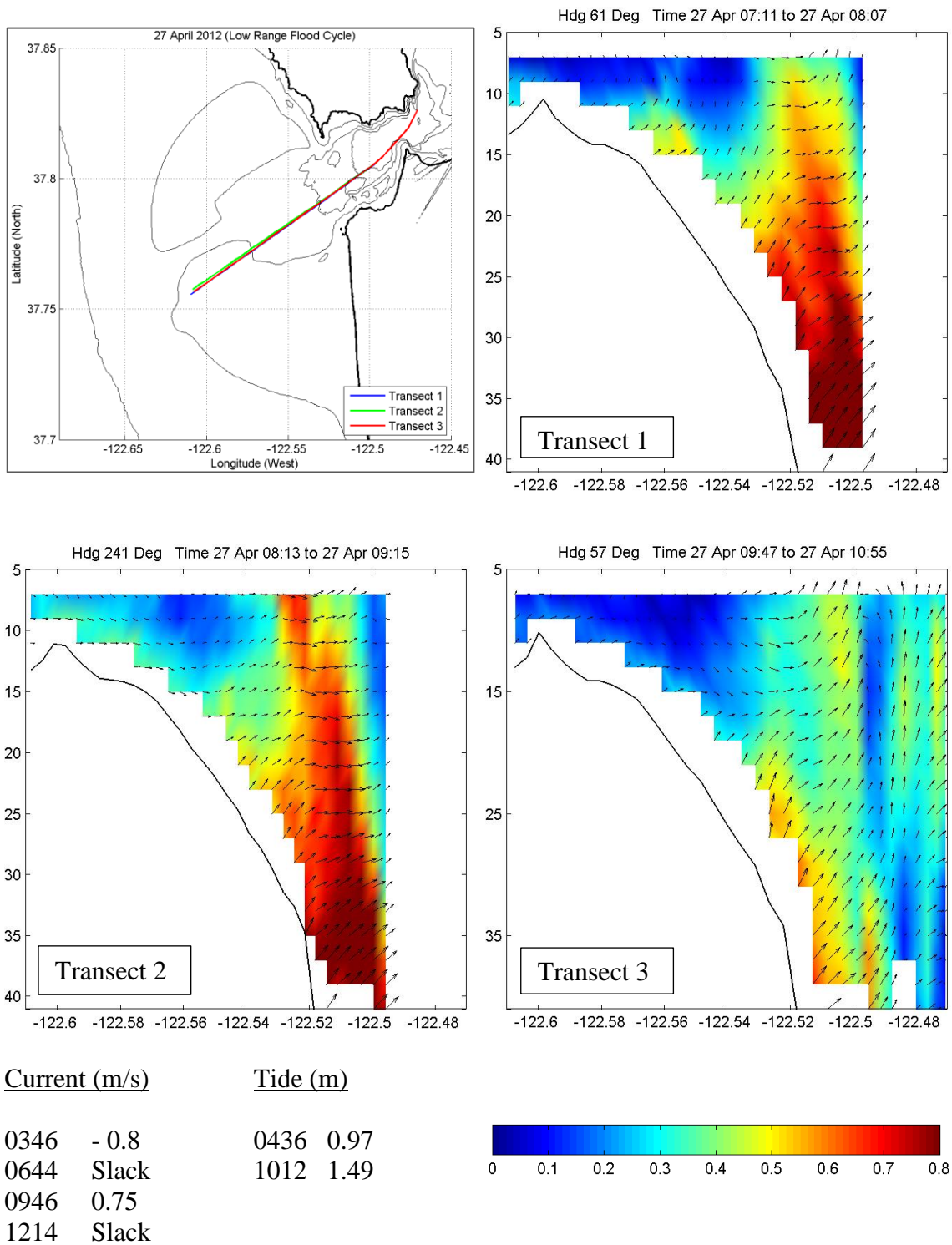


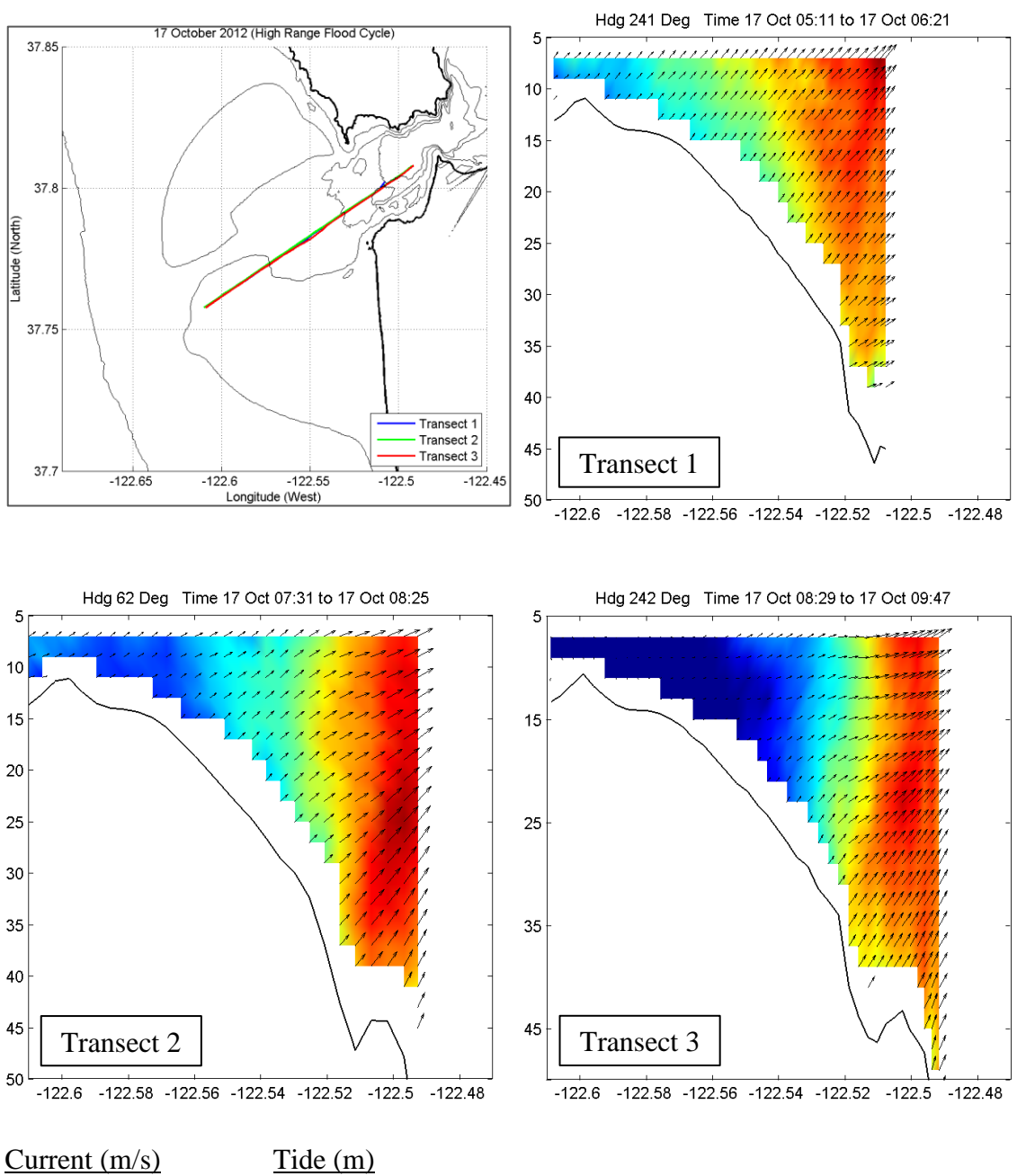
Figure 14. Low Range Flood Cycle (27 April 2012)

2. HIGH RANGE FLOOD

The three transects from October 2012 (spring of new moon) represent a high range flood case where a tidal range of 1.88 m occurred in 7 hours with a maximum predicted current of 2.2 m/s. Transect 1, 2 and 3 (see Figure 15) followed nearly identical tracks along southern side of channel and traversed during the second, fourth and fifth/sixth hours of flood current respectively.

Observed maximum flood current values are less compared to the predicted ones. Unlike the weak currents (low range) case, stronger flood currents are uniformly distributed throughout the water column at any particular location. However, the strength progressively decreases from the deeper channel to shallower areas over the bar. Throughout the flood cycle currents mainly flow in northeast direction.

In this stronger flood cycle, flood currents develop simultaneously along the entire channel right after slack. In shallow areas near bar, the current reaches its maximum value during the second hour of flood current



0411	Slack	0148	-0.3
0712	2.2	0846	1.58
1037	Slack	1343	0.61
1259	-1.6		

Figure 15. High Range Flood Cycle (17 October 2012)

B. EBB CURRENT CASE

1. LOW RANGE EBB

In order to represent the low range ebb, a cycle with a sea level change of 0.3 m during 4.5 hours with maximum predicted current of 0.8 m/s is selected. Transect 1 (see Figure 16) was collected at the peak ebb current (3/4th hour) whereas Transect 2 was collected during last hour of ebb.

The maximum predicted current is in agreement with the observed maximum ebb current. In Transect 1, three distinct regions in the water column are identified. The near surface and bottom currents are of 0.5–0.8 m/s magnitude but flow in opposite direction i.e southwest and north-east, respectively. The mid column portion displays low strength currents (0.1–0.2 m/s) in varying directions.

Towards the last hour of ebb (Transect 2 in Figure 16), the near-surface currents have turned to a southern direction in a counter clockwise (CCW) trend and hence middle band (15–25 m depth) and bottom band (below 25 m) currents have started reversing, flowing in south-easterly and easterly directions respectively. This interesting involving vertical structure scheme, that was not observed during high range ebb discussed below (see Figure 17) may be caused by the inability of the low velocity current to cross the off shore bar and hence recirculating near the bottom. Unfortunately, another complete cycle of low range ebb tidal characteristics is not available to confirm the repeatability of this pattern. However, nearby observations collected during the first hour of a low range ebb current (Transect 3) on 28 April in similar tidal conditions shows 2 similar patterns of ebb currents intensified in the near surface region but currents with insignificant strength in shallow area inshore of bar. In this area, a little bit turning towards south can be seen near the bottom giving an indication of possible reversal of the current.

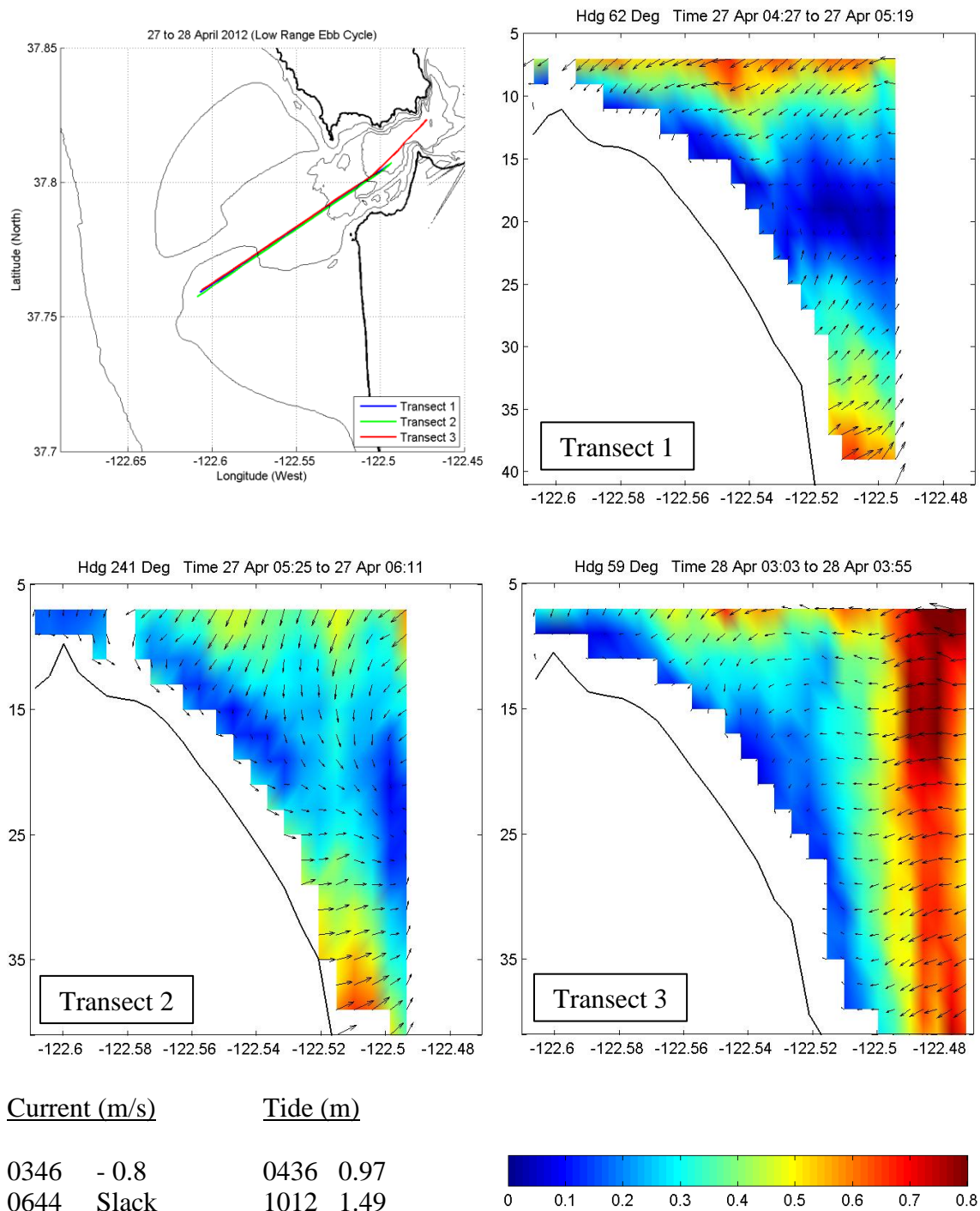


Figure 16. Low Range Ebb Cycle (27 April 2012)

2. HIGH RANGE EBB

The three transects from February 2012 (HHW to LLW cycle) data are selected to represent high range ebb case where sea level decreases by 1.9 m in 7 hours with maximum predicted ebb current of 2.2 m/s. Spatially, the transects (see Figure 17) are spread out latterly across the Golden Gate approaches whereas, temporally, Transect 1, 2 and 3 were traversed during second/third, fifth/sixth and seventh hours of the ebb cycle respectively.

Maximum ebb current values are relatively less compared to the predicted ones. Unlike flood currents, high range ebb currents are surface intensified. Throughout the ebb cycle, currents mainly flow in south-west direction. The strength of current progressively diminishes towards the bottom both near the bar and in the deeper areas near the Golden Gate (Transect 3 in Figure 17), and the vertical variation intensifies during the second hour of the ebb cycle.

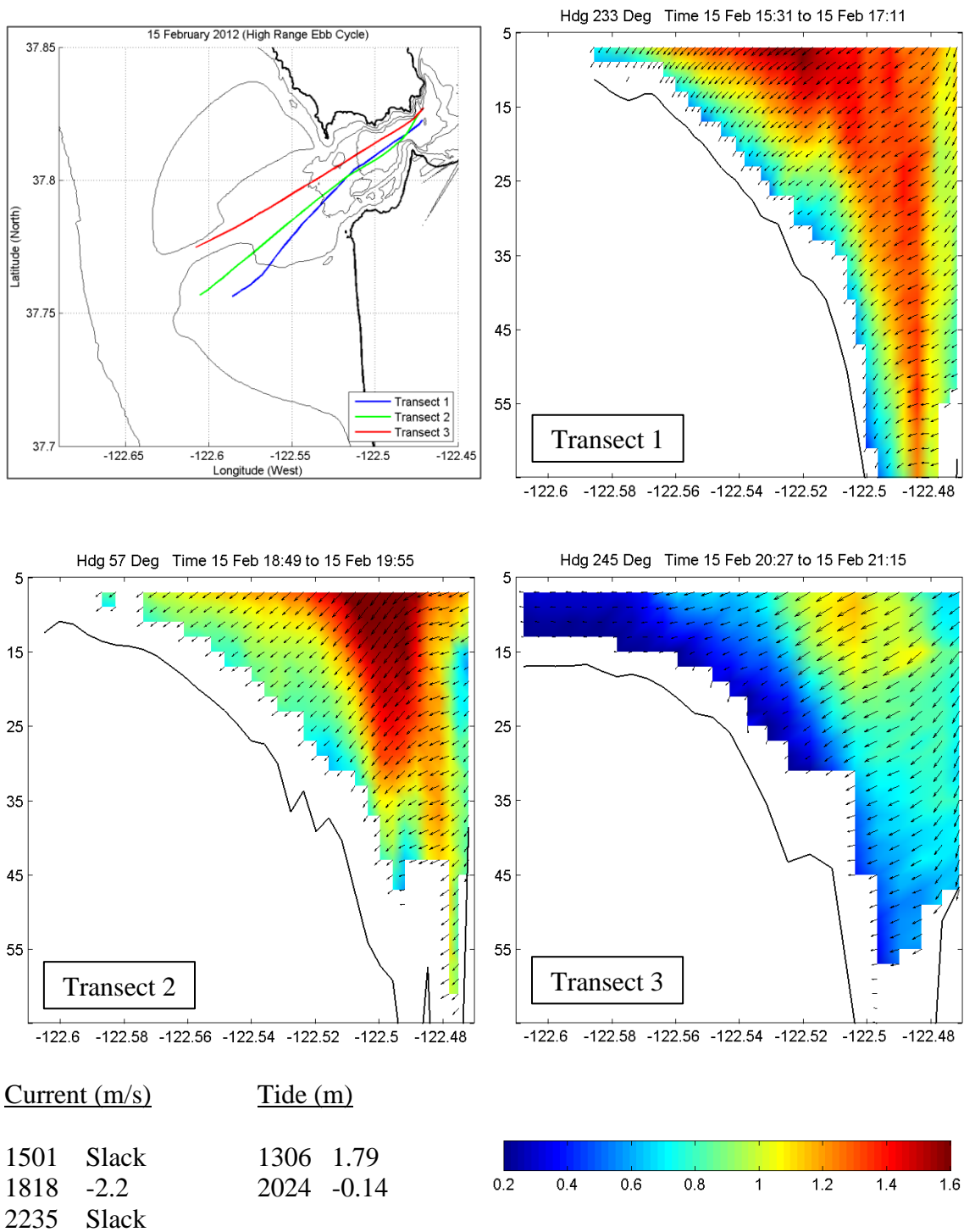


Figure 17. High Range Ebb Cycle (15 February 2012)

C. CROSS-CHANNEL VARIATION IN CURRENT STRENGTH

Apart from temporal variation in current strength, spatial variation i.e variation in both horizontal and vertical planes also affects current strength. Transect 1 and 2 (see Figure 18), which were traversed along the southern and northern sides of the Golden Gate entrance; show the cross-channel variation of strength. The range of flood tide in this case is about 1.3 m occurring over a time span of 6 hours. The much stronger current observed along the southern transect is consistent with the findings of Barnard et al. 2006, who inferred from the orientation of sand wave crests that flood flows predominantly along the southern part of the entrance while ebb results are strongest along the northern part.

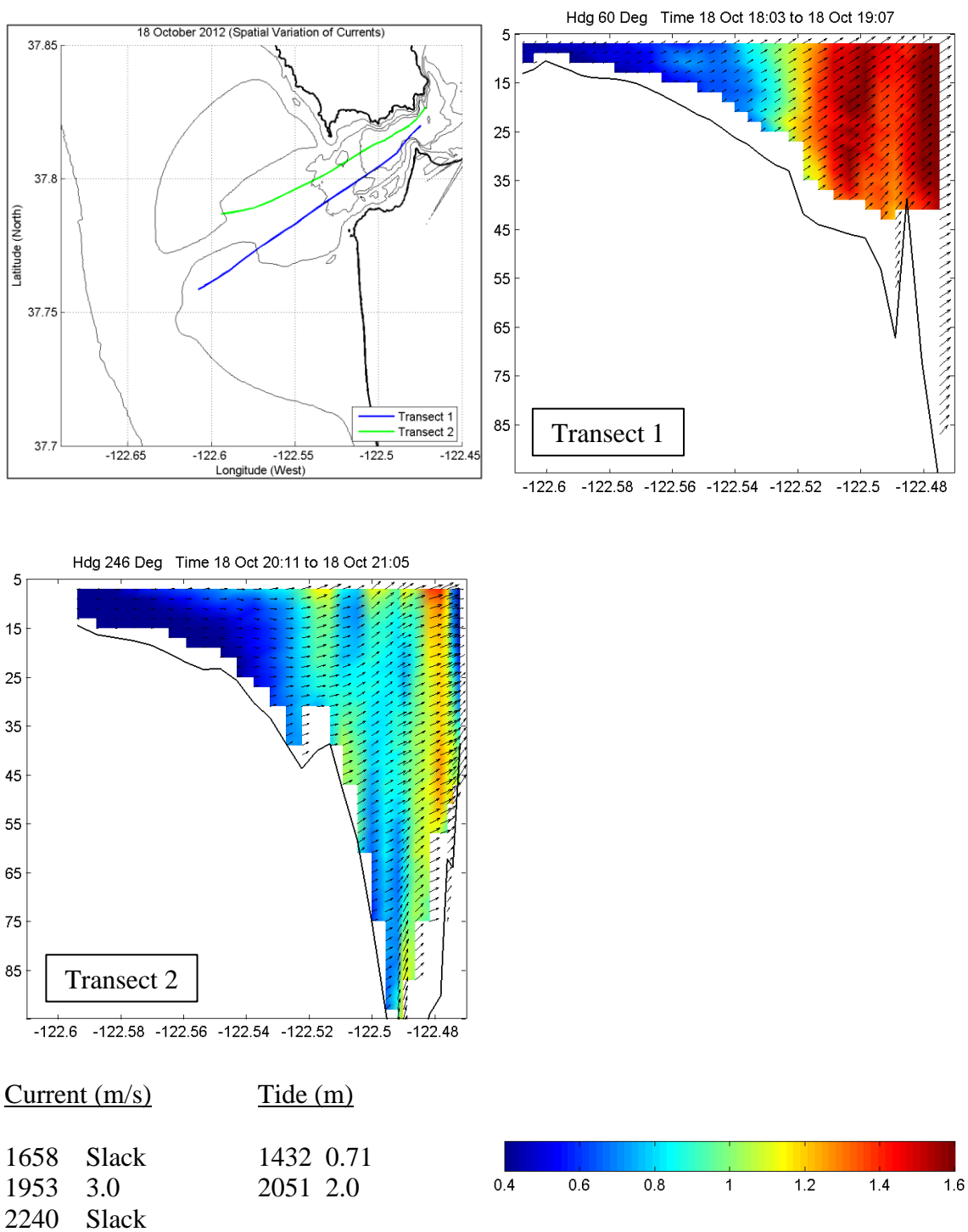


Figure 18. Cross Channel Variation of Currents (18 October 2012)

THIS PAGE INTENTIONALLY LEFT BLANK

V. CONCLUSION

A. SUMMARY

The knowledge of vertical and horizontal structure of currents, especially in coastal regimes, is important for various operational and scientific requirements. In inlets like the entrance to the Golden Gate offshore of San Francisco, the tidal component is dominant and the currents have complex spatial (both horizontal and vertical) and temporal variations as a function of related geography, bathymetry and current generating forces. In these dynamic environments with large waves, strong currents and busy ship traffic, shipboard ADCP is a viable approach for collecting current measurements. ADCP measurements can be collected in regular repeat survey patterns to enable the resolution of tidal harmonic constants and construct the detailed space-time evolution of the current. However, useful results can also be extracted by processing irregularly sampled data collected with a ship of opportunity.

Data used in the study was collected by the R/V Point Sur using a shipboard RDI WH-300 ADCP during four different cruises. UHDAS was used for automatic collection, processing and extraction of data. Information about the vertical structure of tidal currents in the Golden Gate entrance and immediate offshore area was determined from the irregularly sampled data, through the analysis of transects conducting along the channel axis. A Matlab programming code for automatic extraction of transects from overlapping and crossing data tracks was developed for efficiently processing multiple data sets. Selection of start/end of transects is based on abrupt or continuous slow changes in ship's heading and/or speed. As change of speed and heading can be quantified, an automated code in combination with geographic criteria is possible. Maximum allowed change in a ship's speed and heading between the positions of two successive profiles is chosen as primary criteria. Secondary criteria of minimum number of profiles, heading range and maximum/minimum ship's speed are applied to refine the extraction process.

The processed data indicates high degree of reliability of UHDAS operation both in collection and automated processing. Processed data contains many transects traversed in various tidal conditions along various spatial tracks. Out of those, five important cases have been presented in the study. Flood currents are bottom intensified with more strength in the relatively deeper areas near the Golden Gate Bridge. In low tidal range, direction/speed of surface currents varies more than bottom ones whereas, in high tidal range, direction roughly remains uniform throughout the cycle but strength reduces in the direction from the bar to the Golden Gate. Ebb currents are surface intensified with more strength in the relatively deeper areas of channel. In low tidal range, near-surface and bottom currents flow in opposite directions with weak currents in the middle of the water column. In high tidal range, current direction remains uniform throughout the water column during ebb cycle. Current strength exhibits cross channel variation in strength. Ebb results in surface outflow mainly along the northern part of the entrance whereas flood flow shows strength along the southern part. This phenomenon is consistent with previous studies of tidal flow induced sand waves.

B. FUTURE RESEARCH

In order to rigorously validate predicted tidal currents, a special purpose research cruise is required for repeating transects in a regular (temporally and spatially) pattern to carry out harmonic analysis that resolves tidal current constituents. However, the resources for such dedicated research cruises are usually not available whereas research ships can routinely collect ADCP data while conducted other research. While these irregularly sampled data sets are not ideal, they can be very useful for obtaining some tidal current information in areas of interest where in-situ data are scarce. This collected data can be used for two purposes. In the short term, it can be used to check the suitability of hydrodynamic models of the local area and understanding the underlying mechanisms, whereas in the long term, the data can be used to contribute to a large data base of ADCP measurement collected around the globe by ships of opportunity.

LIST OF REFERENCES

- Barth, J. A., & Brink, K. H. (1987). Shipboard Acoustic Doppler Velocity observations near Point Conception: Spring 1983. *Journal of Geophysical Research*, 3925–3943.
- Candela, J., Beardsley, R. C., & Limeburner, R. (1990). Removing Tides from Ship-Mounted ADCP data with application to the Yellow Sea. *Third working conference on current measurement* (pp. 258–266). IEEE.
- Cheng, R. T., & Gartner, J. W. (1984). *Tides, tidal and residual currents in San Francisco Bay, California-Results of measurements 1979–1980, Water-Resources Investigations Report: 84–4339*. U.S. Geological Survey, Water Resources Division.
- Cheng, R. T., & Smith, R. E. (1998). A NOWCAST Model for Tides Tidal Currents in San Francisco Bay, California. *Ocean Community Conference '98* (pp. 537–543). Baltimore, MD: Marine Technology Society.
- Cheng, R. T., Casulli, V., & Gartner, J. W. (1993). Tidal, Residual, Intertidal Mudflat (TRIM) Model and its application to San Francisco Bay, California. *Estuarine, Coastal, and Shelf Science*, Vol. 36, 235–280.
- Conomos, T. J., Smith, R. E., & Gartner, J. W. (1985). Environmental setting of San Francisco Bay. *Hydrobiologia* v.129, 1–12.
- Danilo, C., Chapron, B., Mouche, A., Garello, R., & Collard, F. (2007). Comparisons between HF radar and SAR current measurements in the Iroise sea. *OCEANS 2007- Europe*, 1–5.
- Darwin, G. H. (1962). *The tides and kindred phenomena in the solar system*. San Francisco, California: W. H. Freeman & Co.
- Epler, J., Polagye, B., & Thomson, J. (2010). *Shipboard Acoustic Doppler Current Profiler surveys to assess tidal current resources*. Retrieved from University of Washington website:
http://depts.washington.edu/nnmrec/docs/20100920_EplerJ_conf_MobileADCP.pdf
- Fong, D. A., & Monismith, S. G. (2004). Evaluation of the accuracy of a ship-mounted, bottom-tracking ADCP in a near-shore coastal flow. *Journal of Atmospheric and Oceanic Technology*, 1121–1128.
- Geyer, W. R., & Signell, R. (1990). Measurement of tidal flow around a headland with a shipboard Acoustic Doppler Current Profiler. *Journal of Geophysical Research*, 3189–3197.

- Geyer, W. R., Trowbridge, J. Y., & Bowen, M. M. (2000). The dynamics of a partially mixed estuary. *Journal of Physical Oceanography*, 2035–2048.
- Griffiths, G. (2004). *Current Measurement using ADCP*. Retrieved from National Oceanographic Center Southampton University of Southampton website: www.noc.soton.ac.uk/nmf/usl/gxg/SOES3010_ADCP_Lecture.ppt
- Grove, K. (2001). Background on tides and currents. Retrieved from Department of Geosciences-San Francisco State University website: <http://geosci.sfsu.edu/courses/geol103/labs/estuaries/partIIIA.html>
- Gunawan, B., & Neary, V. S. (2011, September 30). *ORNL ADCP post-processing guide and Matlab algorithms for MHK site flow and turbulence analysis*. Retrieved from ORNL website: <http://www.ornl.gov/sci/waterpower/pdf/TM4042011.pdf>
- Holbrook, J. R., & Frisch, A. (1981). A comparison of near surface CODAR and VACM measurements in the strait of Juan de Fuca, August, 1978. *Journal of Geophysical Research*, 10908–10912.
- Howarth, M. J., & Proctor, R. (1992, May-June). Ship ADCP measurements and tidal models of the North Sea. *Continental Shelf Research*, pp. 601–623.
- King, B. A., Firing, E., & Joyce, T. M. (2001). Shipboard observations during WOCE. *Ocean Circulation and Climate*, 99–121.
- Kosro, P. M. (1985). *Shipboard Acoustic Current Profiling during the Coastal Ocean Dynamics Experiment, SIO Report*. 85–8. La Jolla, California: Scripps Institute of Oceanography.
- Matthews, J. P., Simpson, J. H., & Brown, J. (1988). Remote sensing of shelf sea currents using a high-frequency ocean surface current radar system. *Journal of Geophysical Research*, 2303–2310.
- Introduction to Ocean Currents*. (n.d.). Retrieved from MetEd COMET Program website: <http://www.meted.ucar.edu/oceans/currents/print.htm>
- NEFSC-NOAA. (2006, June 21). *Notes on ADCP principles*. Retrieved from Northeast Fisheries Science Center-Oceanographic Branch NOAA website: http://www.nefsc.noaa.gov/epd/ocean/MainPage/adcp/ADCP_notes.html
- New, A. L. (1992, November–December). Factors affecting the quality of shipboard acoustic Doppler current profiler data. *Deep Sea Research Part A. Oceanographic Research Papers*, 1985–1996.

- NOAA Tides and Currents. (2012). *Physical Oceanographic Real-Time System San Francisco Bay*. Retrieved from NOAA Tides and Currents/San Francisco PORTS website: [http://tidesandcurrents.noaa.gov/ports/ports.shtml?stn=9414290+San Francisco&port=sf](http://tidesandcurrents.noaa.gov/ports/ports.shtml?stn=9414290+San+Francisco&port=sf)
- Physical Oceanography Department, WHOI. (n.d.). *Ocean Instruments: ADCP*. Retrieved from Woods Hole Oceanographic Institution website: <http://www.whoi.edu/instruments/viewInstrument.do?id=819>
- Prandle, D. (1987). The fine structure of nearshore tidal and residual circulation revealed by HF radar surface current measurements. *Journal of Physical Oceanography*, 231–245.
- Poltips-3 Guide* (n.d.). Retrieved from Proudman Oceanographic Laboratory website: <http://www.pol.ac.uk/appl/downloads/PT3guide.pdf>
- Regier, L. (1982). Mesoscale current fields observed with a shipboard profiling Acoustic Current Meter. *Journal of Physical Oceanography*, 880–886.
- Simpson, J. H., Mitchelson-Jacob, E. G., & A. E. Hill. (1990). Flow structure in a channel from and Acoustic Doppler Current Profiler. *Continental Shelf Research*, 589–603.
- Simpson, M. R., & Oltmann, R. N. (1993). *Discharge-measurement system using an acoustic Doppler current profiler with applications to large rivers and estuaries*. Retrieved November 11, 2012, from U.S. Geological Survey Water-Supply Paper 2395: <http://pubs.usgs.gov/wsp/wsp2395/>
- Stacey, M. T., Monismith, S. G., & Burau, J. R. (1999). Measurements of Reynolds Stress profiles in unstratified tidal flow. *Journal of Geophysical Research*, 10933–10949.
- Teledyne RD Instruments. (1996). *ADCP Principles of Operation*. Retrieved from Lamont Doherty Earth Observation-University of Columbia website: http://www.ldeo.columbia.edu/~jkarsten/teach/docs/rdi_primer.pdf
- Terray, E., Gordon, R. L., & Brumley, B. (1997). Measuring wave height and direction using upward-looking ADCPs. *Ocean '97* (pp. 287–290). Halifax, NS, Canada: IEEE.
- Trump, M. (2008, November 5). San Francisco Bay. Retrieved October 9, 2012, from *Wikipedia*: http://en.wikipedia.org/wiki/File:Wpdms_usgs_photo_san_francisco_bay.jpg
- Walters, R. A. (1982). Low Frequency relations in Sea Level Currents in South San Francisco Bay. *Journal of Physical Oceanography*, 658–668.

Walters, R. A., Cheng, R. T., & Conomos, T. J. (1985). Time scales of circulation and mixing processes of San Francisco Bay waters. *Hydrobiologia* v.129, 13–36.

San Francisco Bay (n.d.). Retrieved from *Wikipedia*:
http://en.wikipedia.org/wiki/San_Francisco_Bay

INITIAL DISTRIBUTION LIST

1. Defense Technical Information Center
Ft. Belvoir, Virginia
2. Dudley Knox Library
Naval Postgraduate School
Monterey, California
3. Prof. Thomas Herbers
Department of Oceanography
Naval Postgraduate School
Monterey, California
4. Associate prof. James MacMahan
Department of Oceanography
Naval Postgraduate School
Monterey, California
5. Pakistan Navy Hydrographic Department
Naval Headquarters
Karachi, Pakistan
6. Directorate of Naval Training
Naval Headquarters
Islamabad, Pakistan
7. National Institute of Oceanography
Karachi, Pakistan
8. CDR Muhammad Khalid
PN Hydrographic Department
Liaquat Barracks, Naval Headquarters Karachi
Karachi, Pakistan